ELECTRICAL PROPERTIES OF METAL-DOPED POLYMER MEMBRANES

by

Donald K. F. Lam

Memorandum ERL-M121

25 April 1966

ELECTRONICS RESEARCH LABORATORY

College of Engineering
University of California, Berkeley
94720

Manuscript submitted: 1 October 1965

The research reported herein was supported in part by the Joint Services Electronics Program (U. S. Army, U. S. Navy and U. S. Air Force) under Grant AF-AFOSR-139-65.

ACKNOWLEDGMENT

The author wishes to thank Professors P. O. Vogelhut (Electrical Engineering) and R. A. Wallace (Chemical Engineering) of the University of California, Berkeley, for their advice and helpful discussions. This project was supported by National Science Foundation research grant OSW 14-01-0001-439.

ABSTRACT

The dc electrical conductivities of metal-doped ion-exchange membranes (polystyrenesulfonic acid in a matrix of semicrystalline polyethylene) were measured as a function of temperature from 20 to 100° C in a 50 micron vacuum. Polymer membranes in the hydrogen, sodium, cadmium, and silver forms were prepared for the electrical measurements. Plots of log σ vs 1/T gave straight lines with activation energies characteristic of the ionic forms, ranging from 0.57 to 1.20 eV. Conductivities at 21° C ranged from ~ 10^{-15} Ω^{-1} -cm^{-1} to ~ 10^{-8} Ω^{-1} -cm^{-1}; anisotropy was examined in the silver-doped membrane. Attempts with Hall-effect measurements to determine the sign and concentration of the charge carriers were unsuccessful. Photoconduction studies were carried out with membranes in the cadmium and silver forms. Rise of photocurrent under dc illumination was found to be exponential with time constants of 6.8 and 29 sec for Cd- and Ag-doped samples, respectively. Photocurrent was ohmic up to 400 V and varied linearly with light intensity.

TABLE OF CONTENTS

I. INTRODUCTION

In the past decade, a considerable amount of literature has been published on the electrical properties of organic compounds, some of which have exhibited semiconductive and photoconductive properties. Eley,[1, 2] Inokuchi,[3] Szent-Gyorgyi,[4] and others began to study some organic compounds as semiconductors; Rosenberg's[5] observation of semiconduction in proteins and the possible role of electron-hole picture in photosynthesis[6] has further increased interest in organic materials as semiconductors. Besides their possible contributions to the understanding of energy transfer in biochemical processes, the wide range of electrical characteristics, which can be obtained by varying the chemical composition of organic compounds, may also play a significant role in future electronis technology. Research divisions of General Electric, DuPont, and others are currently evaluating the semiconductive and photoconductive properties of polymers for practical applications.[7, 8] H. A. Pohl of Princeton University has also worked on the semiconduction in polymers.[9]

In this report, the effects of introducing metallic ions into an ion-exchange polymer membrane on its dc conductivity and photoconductive properties are discussed. The starting material is polystyrenesulfonic acid in a matrix of semicrystalline polyethylene and is available as a commercial product from American Machine & Foundry Co. The molecular structure of the material is shown below. The physical structure can be described as an autonomous matrix of linear PSA chains lying loosely among the polyethylene chains.[10]

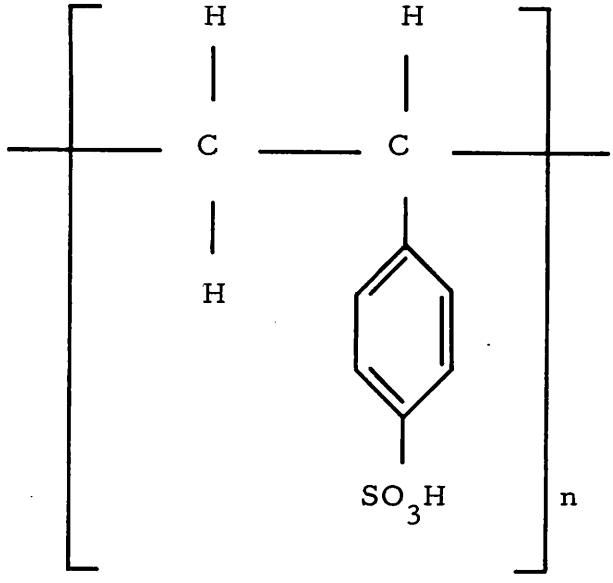

The electrical properties of the polymer membrane in the hydrogen form at various moisture contents have been studied in detail by C. S. Fadley.[11] In this experiment, the hydrogen ion is replaced by Na, Cd, and Ag ions, and all the electrical measurements are made in vacuo. For membranes in the hydrogen form in the wet state, the hydrogen ion is relatively mobile and conduction is thought to involve the actual movement of the hydrogen ion. In the case of the larger and less mobile metallic ion in the dry state, macroscopic transport of the ion seems unlikely, and the conduction mechanism is postulated as due to a random electron-hopping process.[9,12] Results of this experiment are interpreted by this approach.

II. EXPERIMENTAL TECHNIQUES

A. PREPARATION OF SAMPLES

Strips of C-60* (2 × 3 in.), a polystyrenesulfonic cation-exchange membrane, were washed thoroughly with fresh portions of distilled water for several hours. The washed membranes were transformed into the sodium, cadmium, and silver forms by equilibrating in saturated solutions of NaCl, $CdCl_2$, and $AgNO_3$, respectively, and left in the solutions for at least 48 hours. The cations in these solutions replaced the hydrogen ion in the membrane in accordance with:

nRH	+	MX_n	$\rightleftharpoons$	nHX	+	R_nM (1)
PSA membrane		salt soln.		acid		membrane in metallic form.

The acid was removed from the membranes by washing with distilled water. After drying, the strips were cut into sample size with a specially made die and stored in a desiccator. The sample shape and dimensions were as shown in Fig. 1. The electrode contact areas were painted with conductive silver paint to reduce contact resistance.

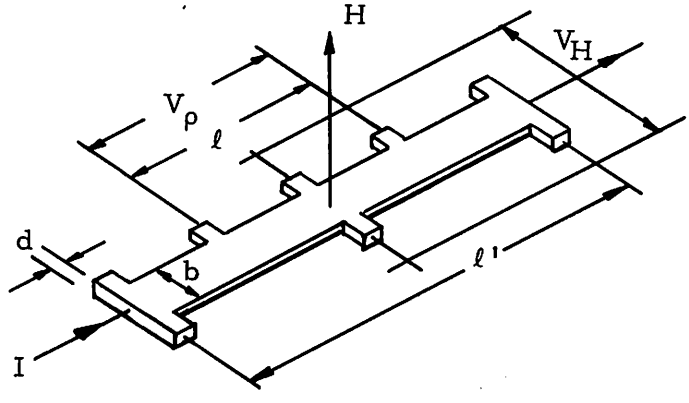

I = 2.40 cm; l' = 3.80 cm; d = 2.67×10^{-2} cm; b = 0.50 cm; V_ρ = voltage across conductivity probes; V_H = voltage across Hall probes; I = current through sample; and H = direction of magnetic field perpendicular to current flow.

Fig. 1. Sample shape.

* Manufactured by American Machine & Foundry Co.

B. CONDUCTIVITY AND HALL-EFFECT MEASUREMENTS

The specimen was mounted on a six-point contact holder made of Teflon as shown in Fig. 2; platinum plated pressure-type contacts were used. Due to the high resistance of the samples, it was necessary to clean and degrease the probes and the Teflon slab with ether. A noninductively wound heater attached to the back of the Teflon block varied the temperature of the sample. A regulated power supply with variable voltage control was used to operate the heater. Temperature was measured with thermocouples and an L & N 8692-169 potentiometer. The complete specimen holder was enclosed in a brass chamber which fitted into a 3/4-in. gap of a 6-in. Varian-type V-4007 magnet provided with a regulated power supply. The maximum field available was 7.5 kG. The chamber could be evacuated to approximately 50 microns. An Amphenol connector was used to make connections between the sample holder and the instruments; later in the experiment, it was necessary to replace the Amphenol connector with BNC connectors to improve the insulation resistance. In addition to the shielding provided by the brass chamber, Amphenol low-noise cable (Nos. 21-537) was used to make all connections to minimize stray effects. The ac pickup, as measured by an oscilloscope, was less than 0.002 V peak-to-peak. Current to the sample was supplied by a shielded battery. Currents and voltages were measured with a set of calibrated resistors and a Cary 31 vibrating reed electrometer which had an input impedance of 10^{14} ohms. The three-probe method[13] for Hall-effect measurements was employed. The system schematic and apparatus used were as shown in Figs. 3 and 4.

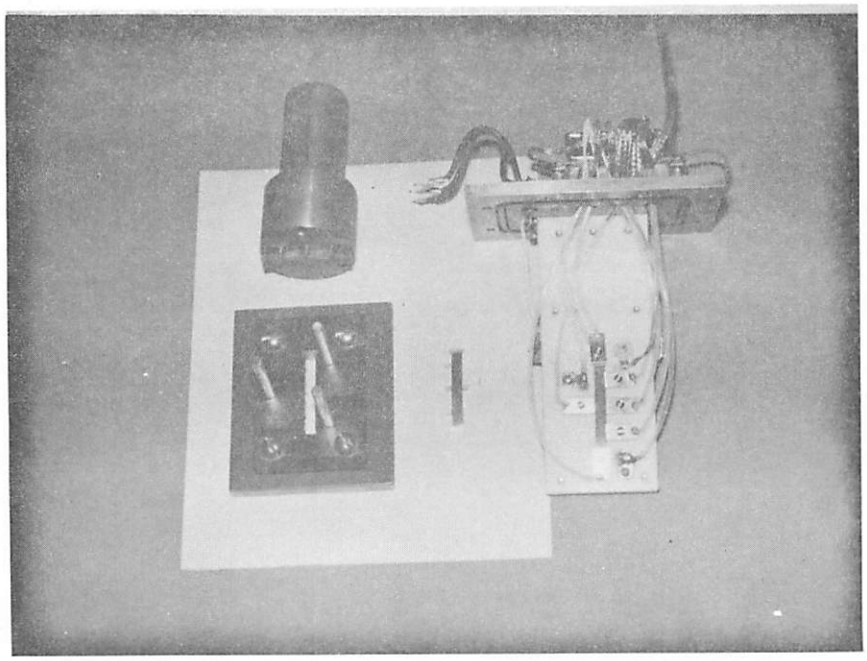

Fig. 2. Cutting die and sample holder for conductivity and Hall measurements.

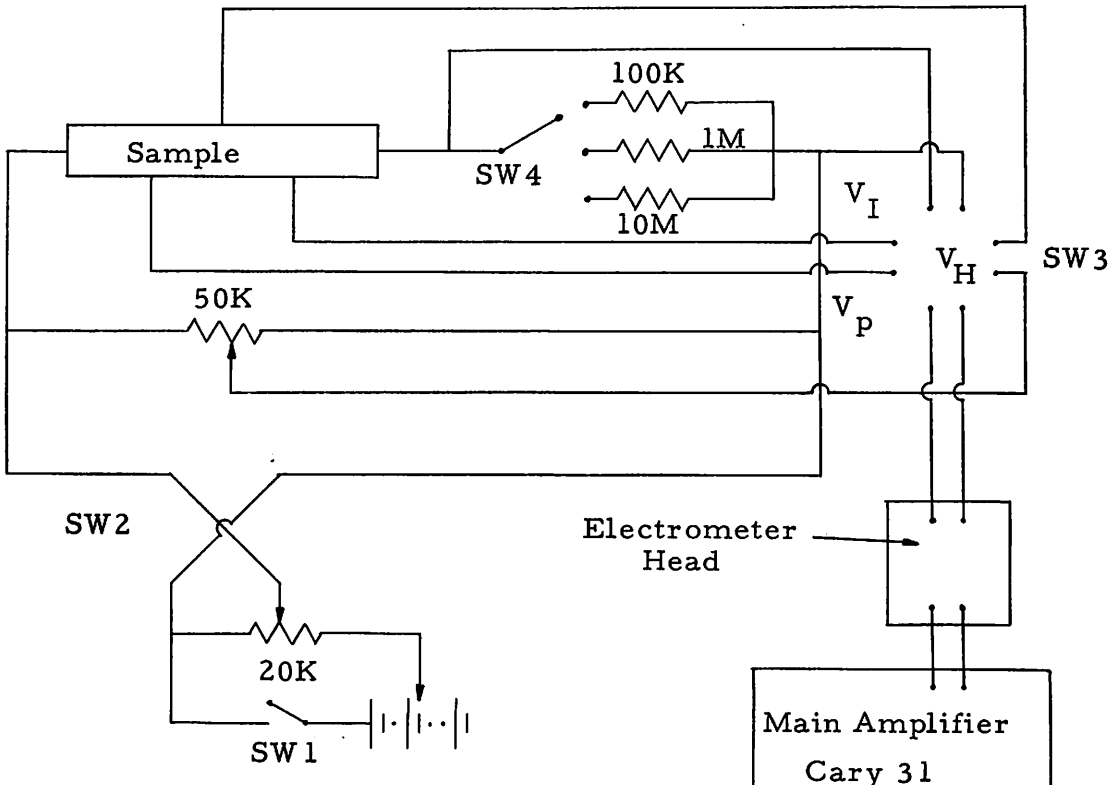

SW1 - battery switch
SW2 - field reversing switch
SW3 - selector switch
SW4 - current range selector

Fig. 3. Schematic for conductivity and hall measurement.

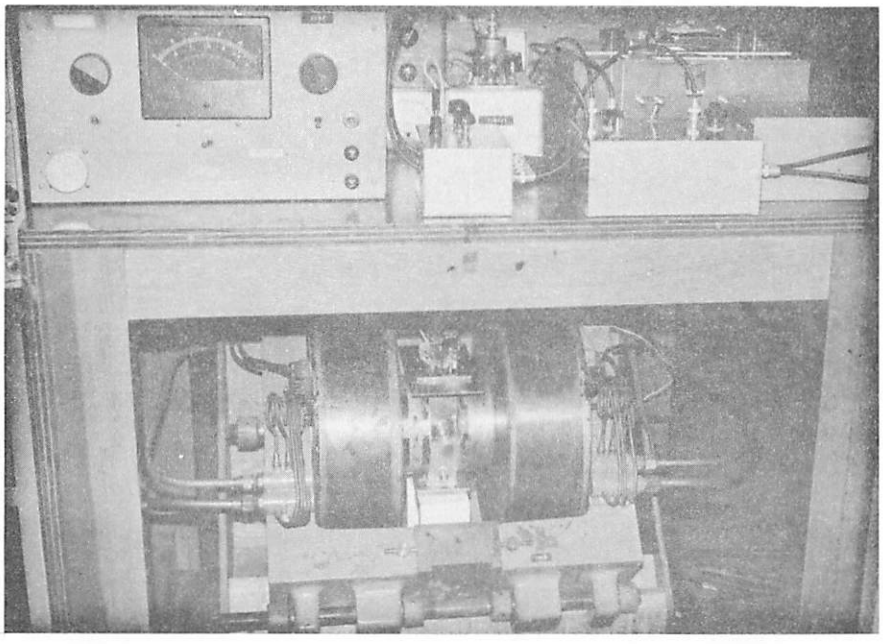

Fig. 4. Apparatus for conductivity and Hall measurements.

For conductivity measurements, the four-probe method was chosen to eliminate undesirable contact resistance at the current electrodes. However, the four-probe measurements became difficult to carry out when the current through the sample dropped below 10^{-9} amp due to pickup problems. It was then necessary to ground one side of the battery to improve stability. Because the Cary electrometer did not have a grounded input, it was replaced by a Keithley 610B in the two-probe method.

The dc conductivity was measured over a temperature range of 20 to 100° C. Two hours were allowed between temperature changes to allow the sample to return to thermal equilibrium. In cases where current decreased with time, the current measurements were taken one minute after the voltage was applied.

C. CONDUCTIVITY ANISOTROPY AND PHOTOCONDUCTIVITY MEASUREMENTS

As shown in Fig. 5, a different sample holder was constructed for this set of experiments. Two copper-disc electrodes were mounted on Teflon-insulated supports. Each disc could be heated individually by a 25-W, 10-ohm Silicohm resistor. Thermocouples were attached to the electrodes at positions close to the sample. The thermocouple wires were shielded to reduce noise. By a set of clamps fitted to the discs, the membrane specimen could be mounted in three different orientations to study conductivity anisotropy and photoconduction experiments. Referring to Figs. 6 and 7, configuration (a) was used to measure photoconductivity and dark conductivity in the σ_1 direction, (b) and (c) were used to measure dark conductivity in the σ_2 and σ_3 directions, respectively. The electrode assembly was enclosed in a cylindrical outer case with windows and could be evacuated to 50 microns. Illumination for the photoconduction experiments was provided by an AO No. 353 lamp with a focusing condensing system and a variable voltage transformer to control the light intensity. Light intensity was measured with an

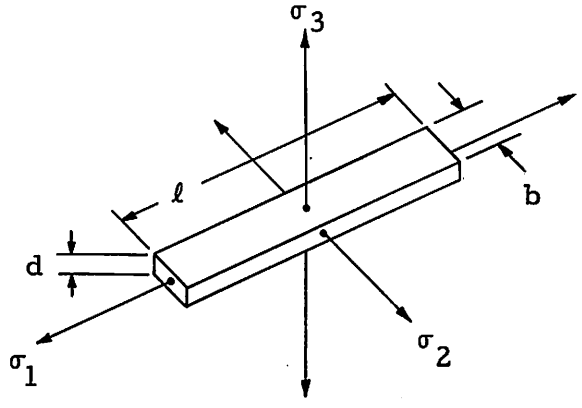

σ_1 = Direction of highest conductivity

σ_2 = Direction of intermediate conductivity

σ_3 = Direction of lowest conductivity

Fig. 5. Conductivity anisotropy.

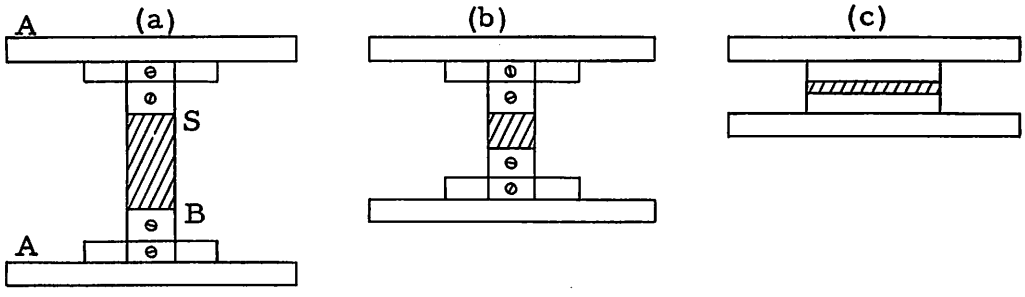

A - disc-shaped copper electrode
B - clamps fitted to the electrode A
S - sample

Fig. 6. Configurations of sample mounting.

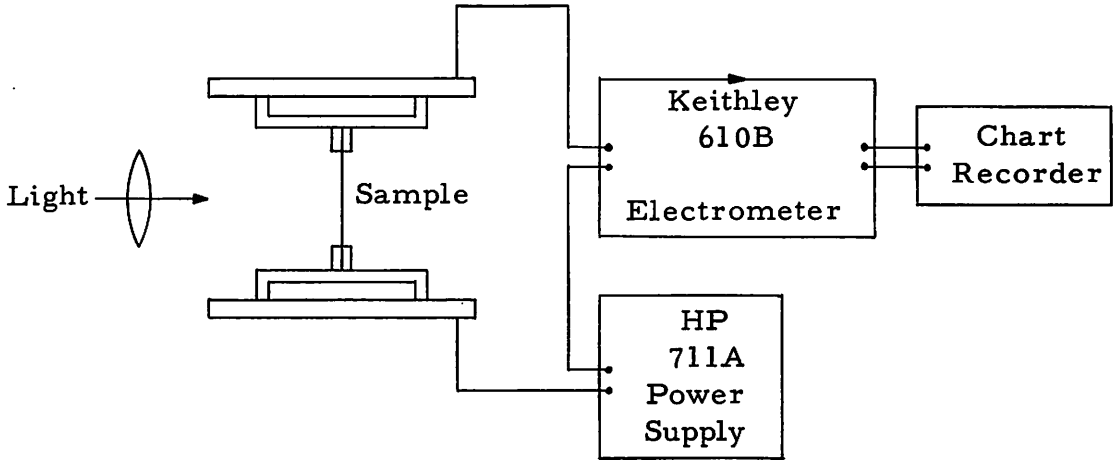

Fig. 7. Schematic for photoconductivity measurement.

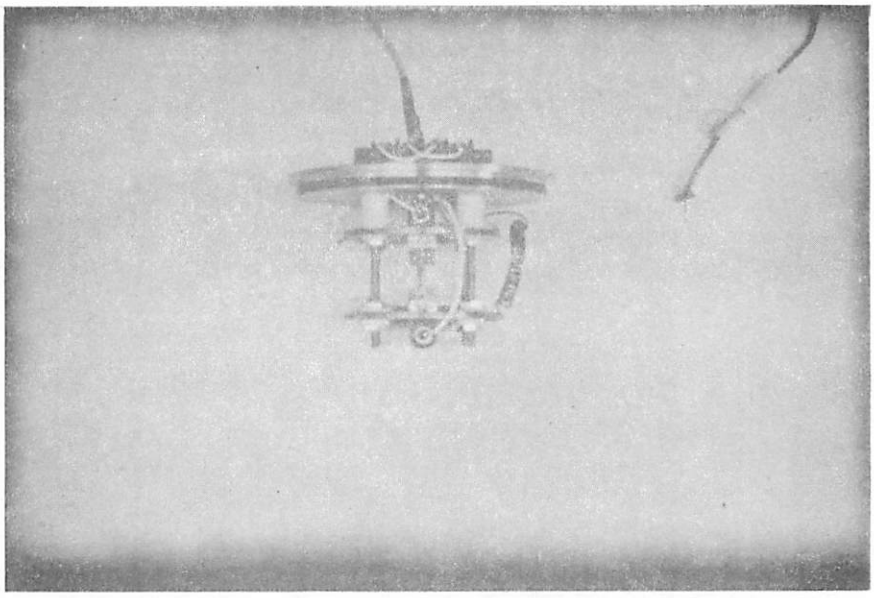

Fig. 8. Sample holder for photoconductivity measurement.

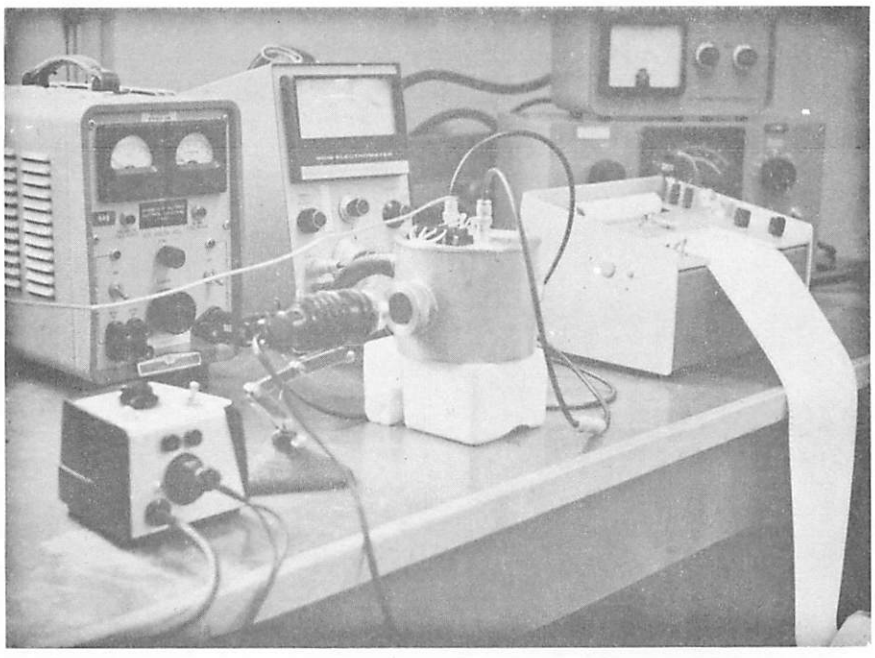

Fig. 9. Apparatus for photoconductivity measurement.

Optics Technology Inc. power meter 610. An HP 711A power supply provided applied voltage across the sample; current was measured with the Keithley 610B electrometer. To record the rise and decay of the photocurrent, the output of the electrometer was fed into a Nesco JY110 charge recorder. Figures 8 and 9 show the apparatus used for this part of the experiment.

III. EXPERIMENTAL RESULTS

A. CONDUCTIVITY MEASUREMENTS

Conductivity measurements were performed on membranes in the H, Na, Cd, and Ag forms. The specific conductivity σ was calculated from the expression:

$$\sigma = \frac{I\ell}{V_\rho db} \text{ ohm}^{-1}\text{-cm}^{-1}, \tag{2}$$

where

I = current through sample in amps,

V_ρ = voltage drop across conductivity probes in volts,

ℓ = length of sample between conductivity probes in cm,

b = width of sample in cm,

d = thickness of sample in cm.

Plots of log σ vs $1/T$ gave straight lines and showed that the materials obeyed the standard law of semiconduction:

$$\sigma = \sigma_o \exp(-E/kT), \tag{3}$$

where

σ_o = pre-exponential constant characteristics of sample in Ω^{-1}-cm^{-1},

E = activation energy in eV,

k = Boltzmann's constant,

T = temperature of sample in ^{o}K.

The activation energy E was calculated from the slope of log σ vs 1/T graphs as

$$E = -1.98 \times 10^{-4} \left(\frac{\Delta \log \sigma}{\Delta \frac{1}{T}} \right) . \qquad (4)$$

The constant σ_o was calculated from (2) by substituting in the calculated value of E and the observed value of σ at a given temperature. The "wet" conductivities for samples equilibrated at 21° C and 42% R. H. were also calculated for comparison. The results are summarized in Table 1. Plots of log σ vs 1/T of the various samples are in Figs. 10 to 14.

Reproducibility of the values of E were bood but the currents were not; deviations between different samples varied as much as one order of magnitude. The same kind of discrepancy was observed by others working with anthracene[14] and molecular complexes.[15]

The subsequent conductivity vs 1/T characteristics of heating a Na-doped sample to 131° C, i.e., above the transition temperature T_g of polyethylene, are shown in Fig. 12. The net effect was to increase the resistivity, while the activation energy remained the same. Reexamination of the specimen showed changes in texture and color.

B. HALL-EFFECT MEASUREMENTS

Noise and capacitively coupled drift made Hall signal detection difficult. The sensitivity of the experimental setup was able to observe signals greater than 20 μV, but no Hall signal of this magnitude was detected with the maximum attainable field of 7.5 kG.

Table 1.

Electrical Characteristics of Metal-Doped Polymer Membranes

$$\sigma = \sigma_0 \exp(-E/kT)\ \Omega^{-1}\text{-cm}^{-1}$$

Ionic Form	Sample No.	$\sigma^{*}\ \Omega^{-1}\text{-cm}^{-1}$	$\sigma^{1}\ \Omega^{-1}\text{-cm}^{-1}$	E, eV	$\sigma_0\ \Omega^{-1}\text{-cm}^{-1}$
H	H - 1	2.62×10^{-5}	3.04×10^{-8}	0.78	5.42×10^{5}
	H - 2	2.49×10^{-5}	4.25×10^{-9}	0.81	2.29×10^{5}
Na	Na - 1	1.68×10^{-5}	3.37×10^{-9}	0.82	2.95×10^{5}
	Na - 2	-------	3.55×10^{-10}	0.88	3.68×10^{5}
See Note (a)	Na - 3	-------	9.00×10^{-12}	0.86	4.92×10^{3}
Cd	Cd - 1	1.10×10^{-7}	--------		
See Note (b)	Cd - 2	-------	$\sim 1.0 \times 10^{-15}$	1.20	2.64×10^{5}
Ag	Ag - 1	2.00×10^{-5}	6.60×10^{-9}	0.57	2.52×10^{2}
	Ag - 2	1.71×10^{-5}	1.27×10^{-8}	0.60	2.06×10^{2}

Note:

σ^{*} - sample equilibrated at 21°C and 42%R.H.

σ^{1} - sample equilibrated at 21°C and 50 micron vacuum

a - measurements were made after heating Sample No. Na - 2 to 131° C

b - conductivity for Sample No. Cd - 2 was measured in the σ_3 direction, sample resistance exceeded the leakage resistance of the apparatus in the σ_1 and σ_2 directions

All conductivities were measured in the σ_1 direction unless specified otherwise.

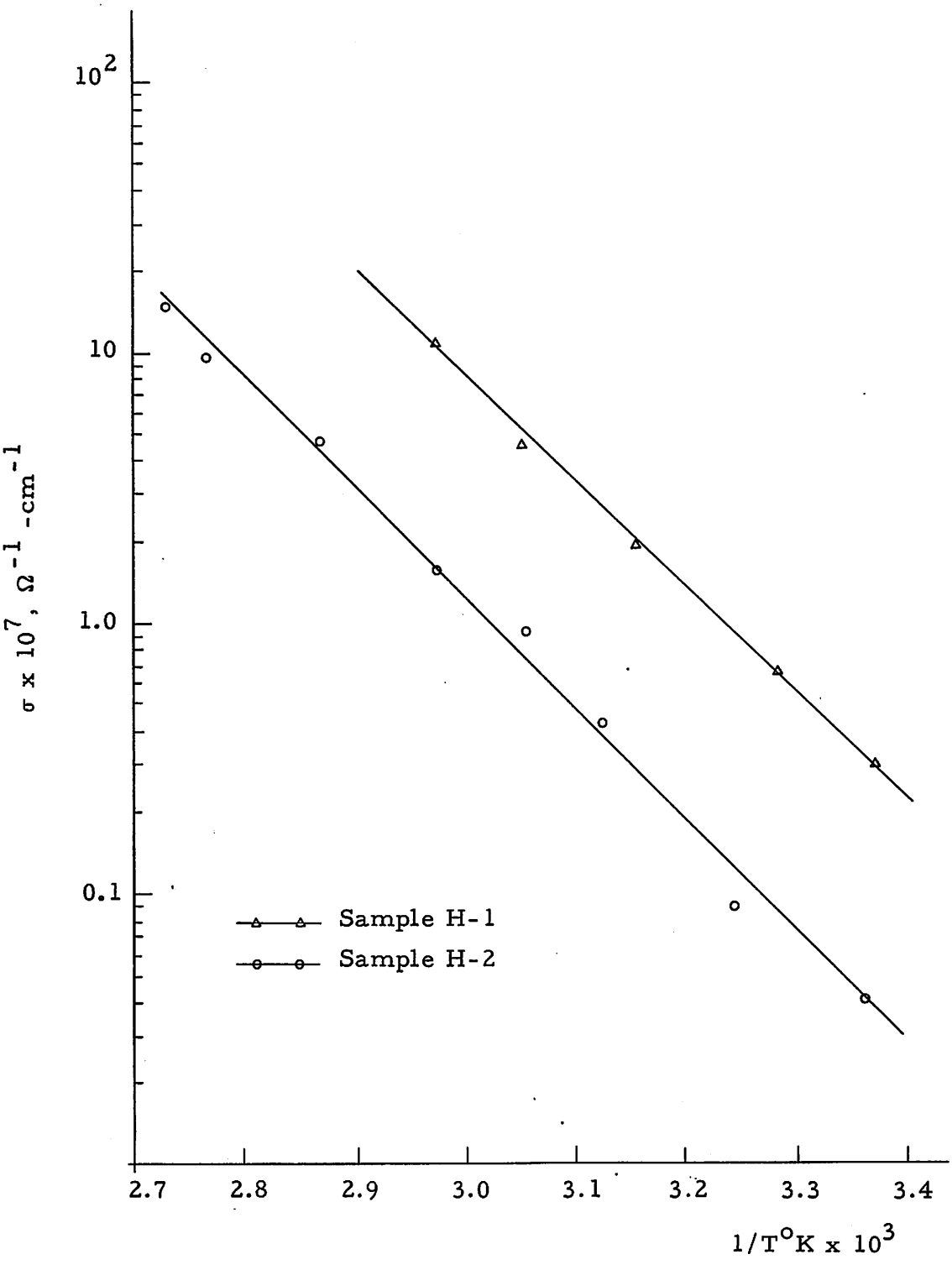

Fig. 10. Conductivity vs temperature in metal-free polymer membrane (hydrogen form)

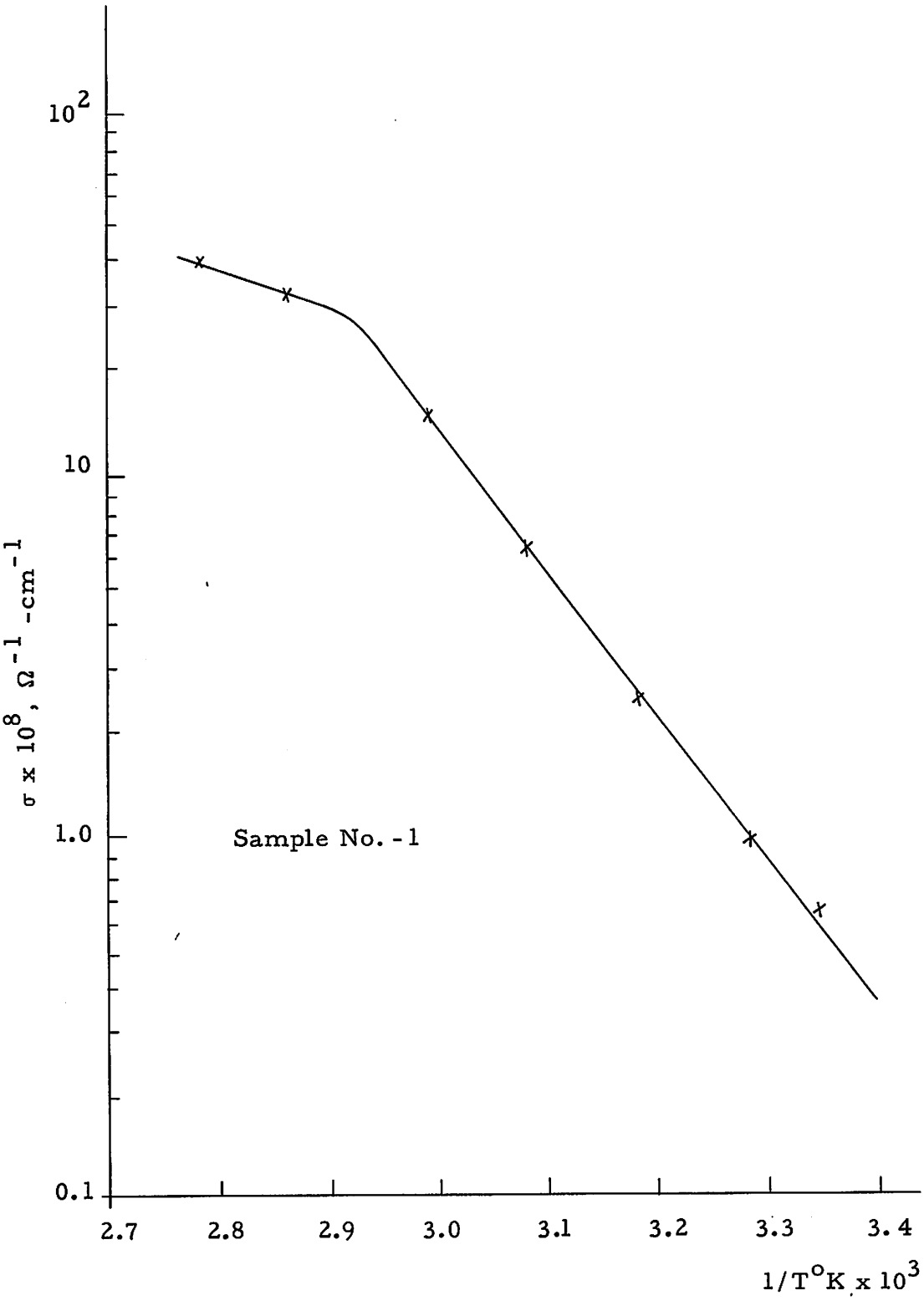

Fig. 11. Conductivity vs temperature in Na-doped membrane

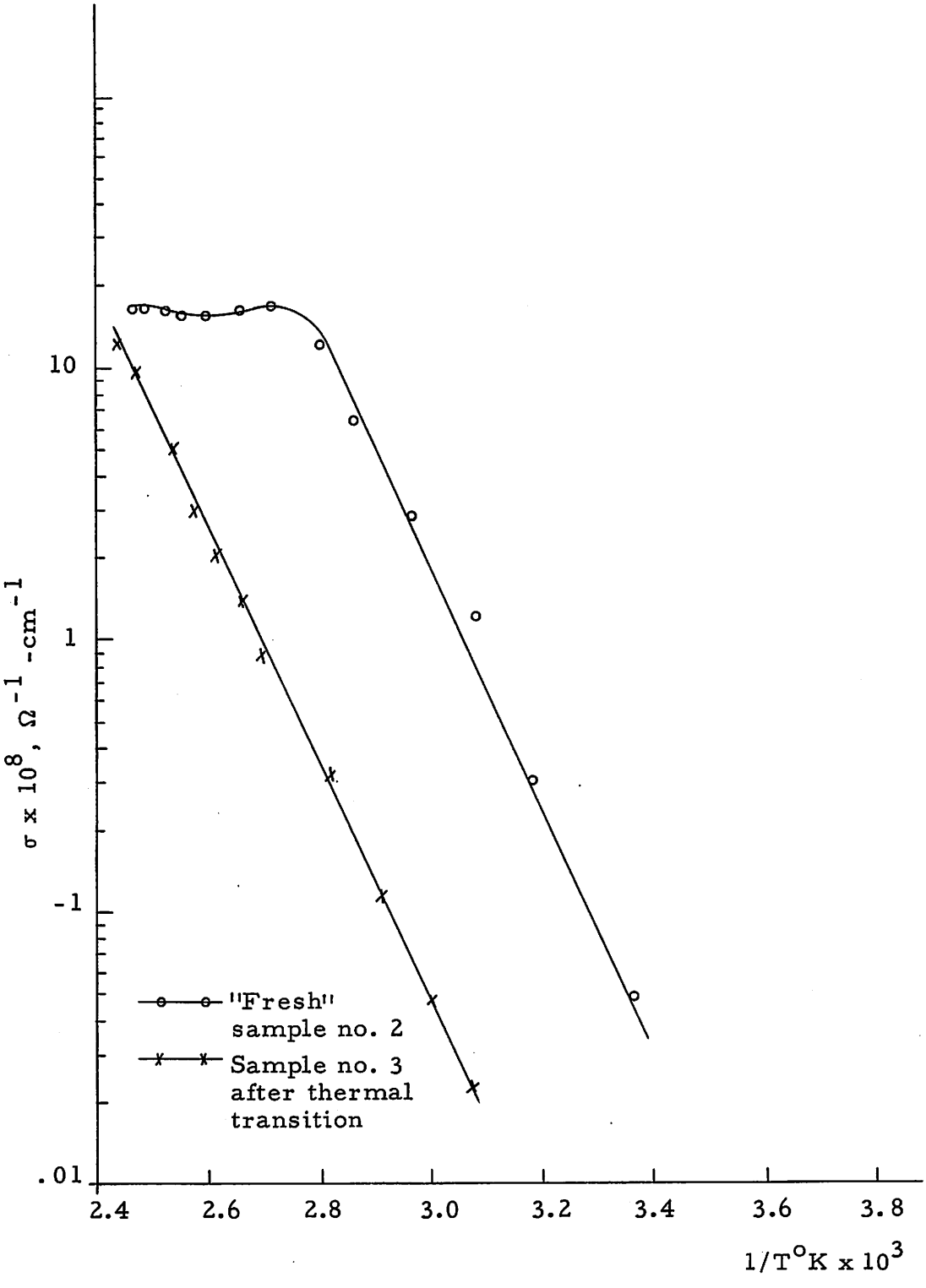

Fig. 12. Effect of heating a Na-doped membrane over the Tg temperature of polyethylene

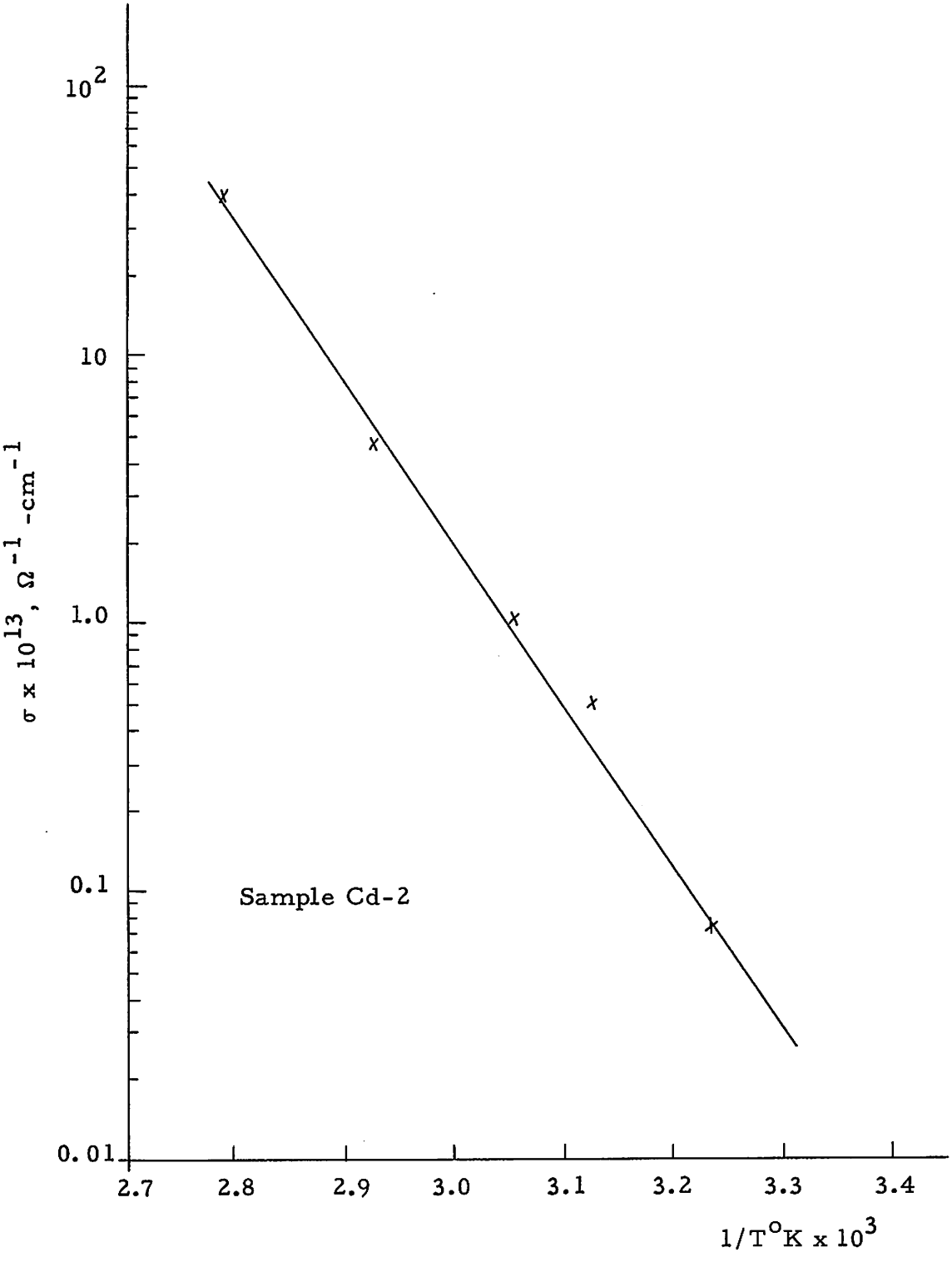

Fig. 13. Conductivity vs temperature in Cd-doped membrane.

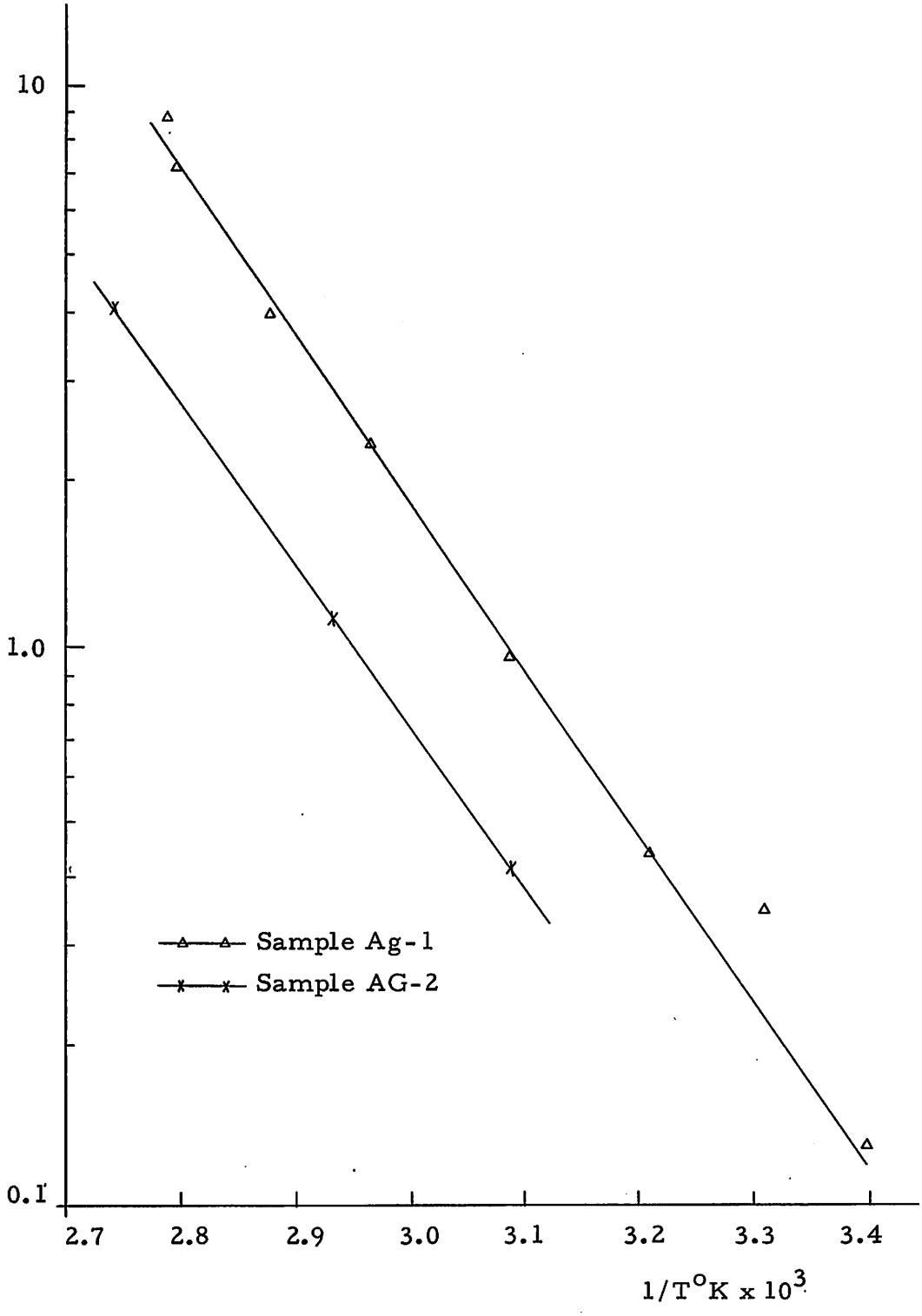

Fig. 14. Conductivity vs temperature in Ag-doped membrane.

C. OBSERVED CURRENT AS A FUNCTION OF TIME

On application of an applied voltage across the sample, the initial current was about one order of magnitude higher than the steady-state value and decayed in time. The steady state was reached more quickly at higher temperatures and for samples with higher conductivities. This time dependence of conduction current was most prominent in Cd-doped samples. The current-vs-time characteristics for the Cd-doped sample at 46.5 and 85° C are shown in Fig. 15 (a) and (b).

This behavior was typical of insulators with traps; a similar phenomen was observed in CdS crystals[16] and napthalene.[17] When an electric field was applied to a high resistivity material with ohmic electrodes, electrons were injected into the conduction band.[18] If trapping centers were present in the material, these electrons became trapped and negative space charge would build up, decreasing the current and setting up a back e.m.f. Such a back e.m.f. was observed by discharging the sample. This result suggested that the cadmium ionic sites acted as traps for electrons.

D. CONDUCTIVITY ANISOTROPY IN Ag-DOPED MEMBRANE

The electrical conductivity of a Ag-doped membrane was measured along the directions as indicated in Fig. 6, and the results are tabulated in Table 2. Plots of log σ vs 1/T are shown in Fig. 16.

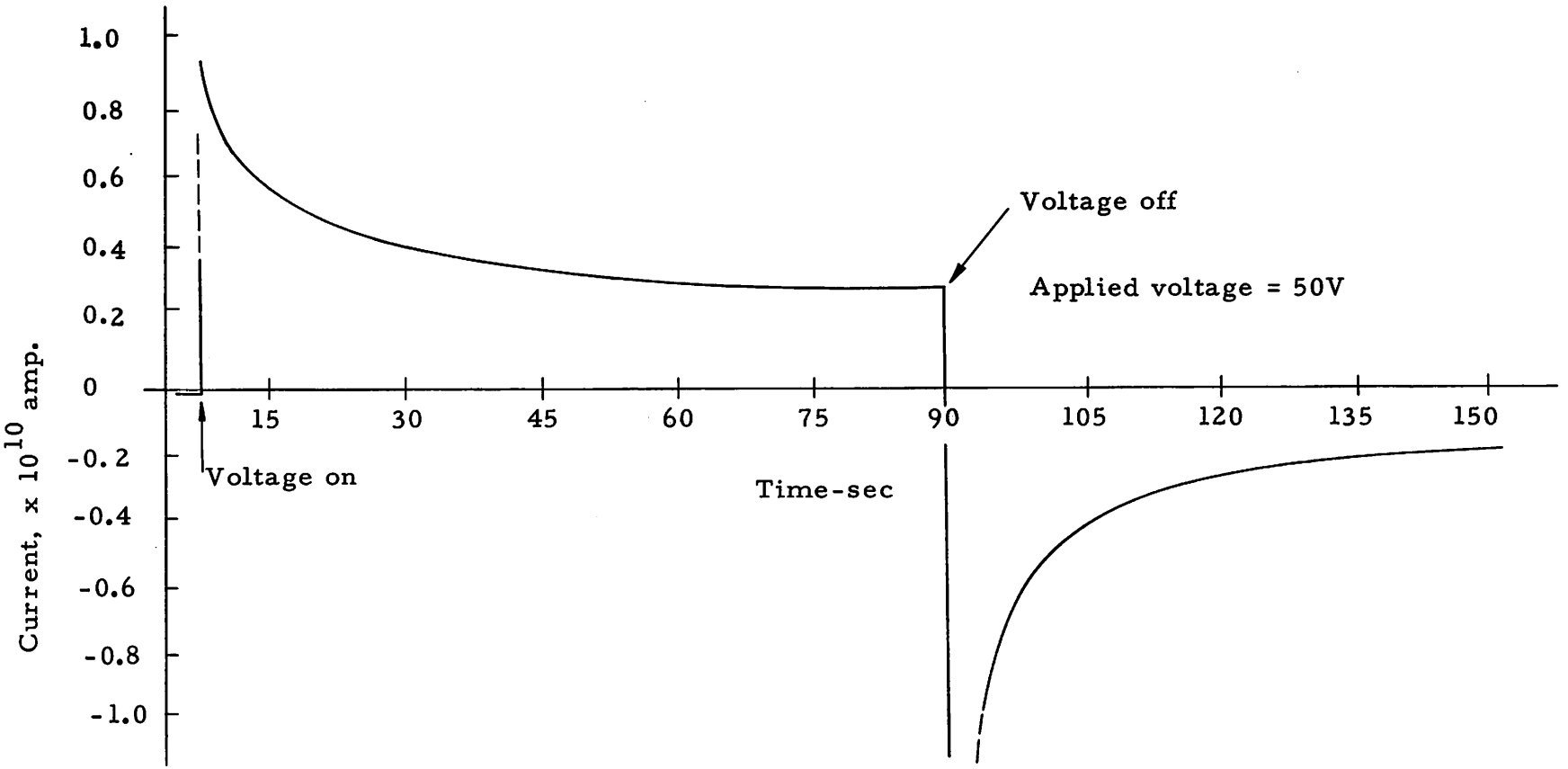

Fig. 15(a). Time dependent current in Cd-doped membrane at 46.5°C.

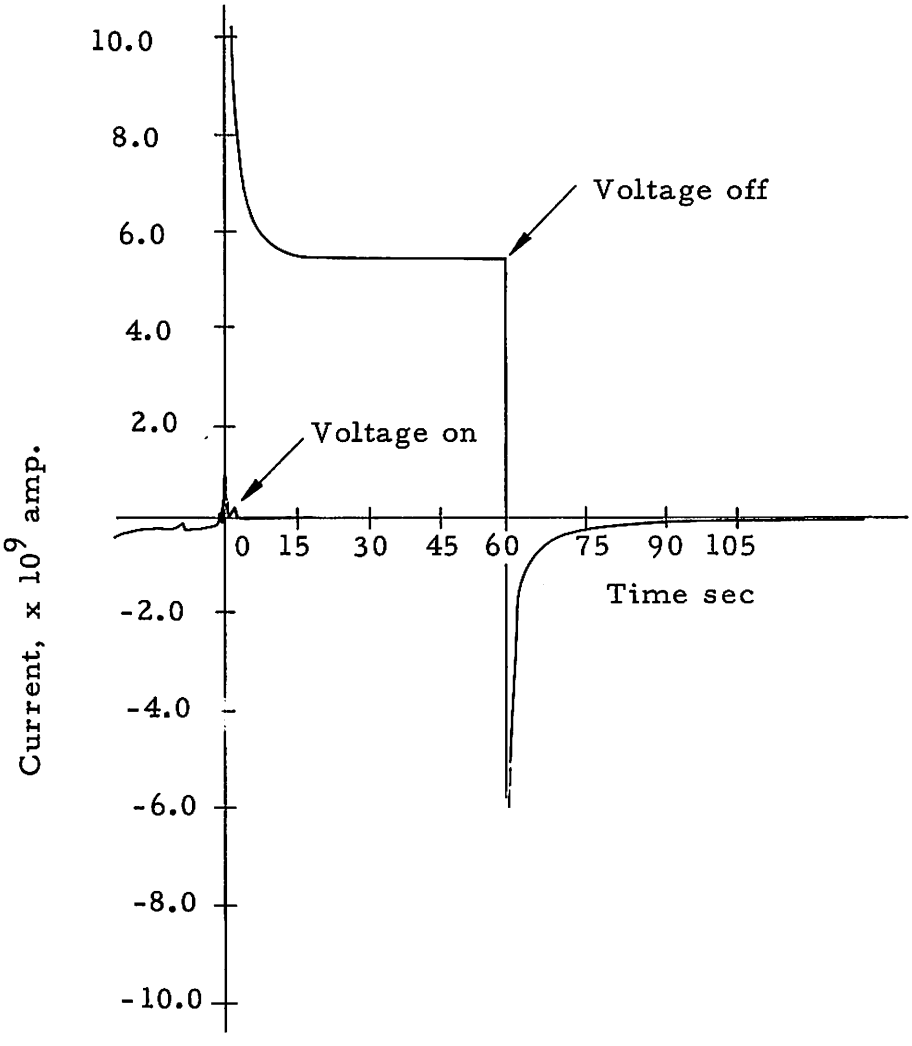

Fig. 15(b). Time dependent current in Cd-doped membrane at 85°C.

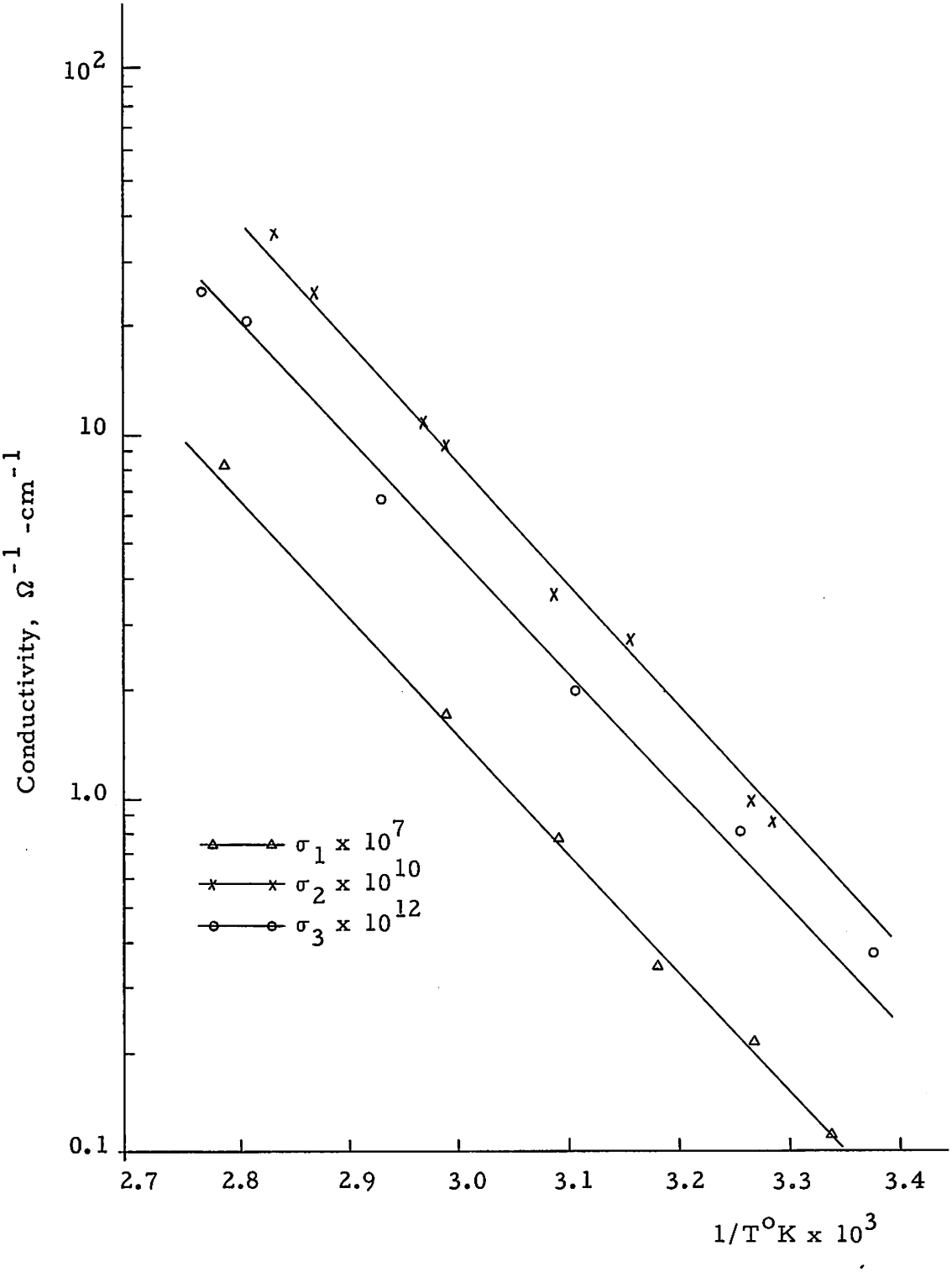

Fig. 16. Conductivity anisotropy in Ag-doped membrane.

Table 2.

Conductivity Anisotropy in Ag-Doped Membrane

Direction of Current Flow	E, eV	$\sigma_0\ \Omega^{-1}\text{-cm}^{-1}$	$\sigma_{21^\circ C}$
σ_1	0.65	8.74×10^{2}	7.70×10^{-9}
σ_2	0.67	1.18×10	3.94×10^{-11}
σ_3	0.65	3.09×10^{-2}	2.46×10^{-13}

Since E remained constant, the anisotropic effect can be taken care of by including a geometric factor in the pre-exponential term:

$$\sigma_1 = k_1 \sigma_0 \exp(-E/kT), \qquad (5)$$

$$\sigma_2 = k_2 \sigma_0 \exp(-E/kT), \qquad (6)$$

$$\sigma_3 = k_3 \sigma_0 \exp(-E/kT). \qquad (7)$$

Choosing $k_1 = 1$, $\sigma_0 = 8.74 \times 10^{2}$, we have

$$k_2 = 1.35 \times 10^{-2},$$

$$k_3 = 3.53 \times 10^{-5}.$$

E. PHOTOCONDUCTIVITY MEASUREMENTS

Photoconductivity measurements were performed on the membranes in the Ag and Cd forms. The response of conduction current under dc illumination for the Ag-doped membrane was as shown

in Fig. 17. When the light was turned on, the current rose exponentially with a time constant of 29 sec, and reached a steady-state in about 150 sec. After the light was turned off, the photo-generated carriers recombined and the decay of conduction current was again exponential. The rise of conduction current under illumination was found to be:

$$i(t) = I_D + I_{ph}(1 - e^{-t/\tau}) . \tag{8}$$

The decay of condution current after the light was turned off followed the expression

$$i(t) = I_D + I_{ph}\, e^{-t/\tau} , \tag{9}$$

where

I_D = steady state dark conduction current,

I_L = steady state illuminated current,

I_{ph} = steady state photocurrent = $I_L - I_D$,

τ = time constant.

The photoconduction characteristics of the Ag-doped membrane as a function of light intensity is shown in Table 3 and plotted in Fig. 18. Photocurrent was found to vary linearly with light intensity.

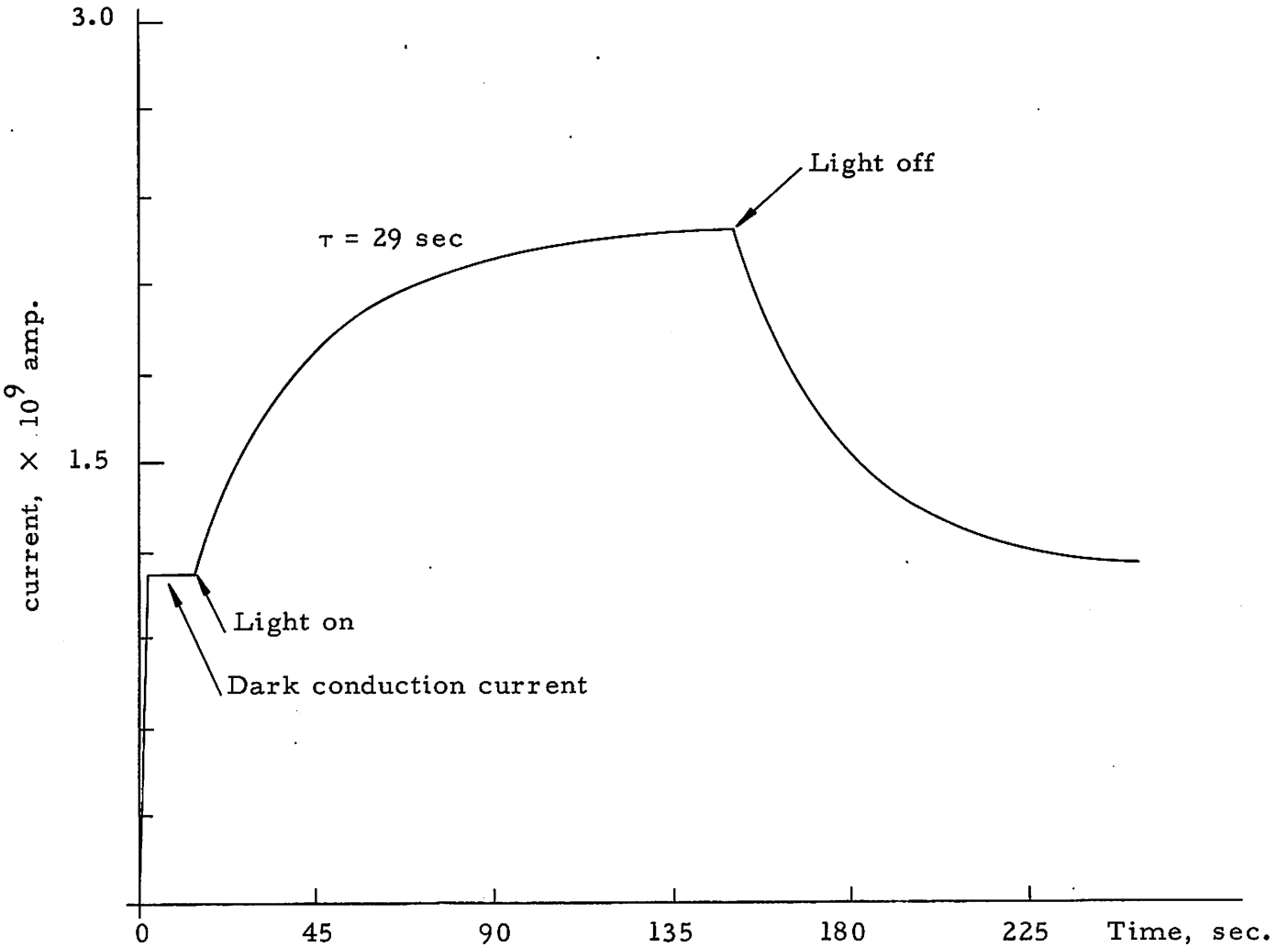

Fig. 17. Response of photocurrent in Ag-doped polymer membrance under dc illumination (in 50μ vacuo).

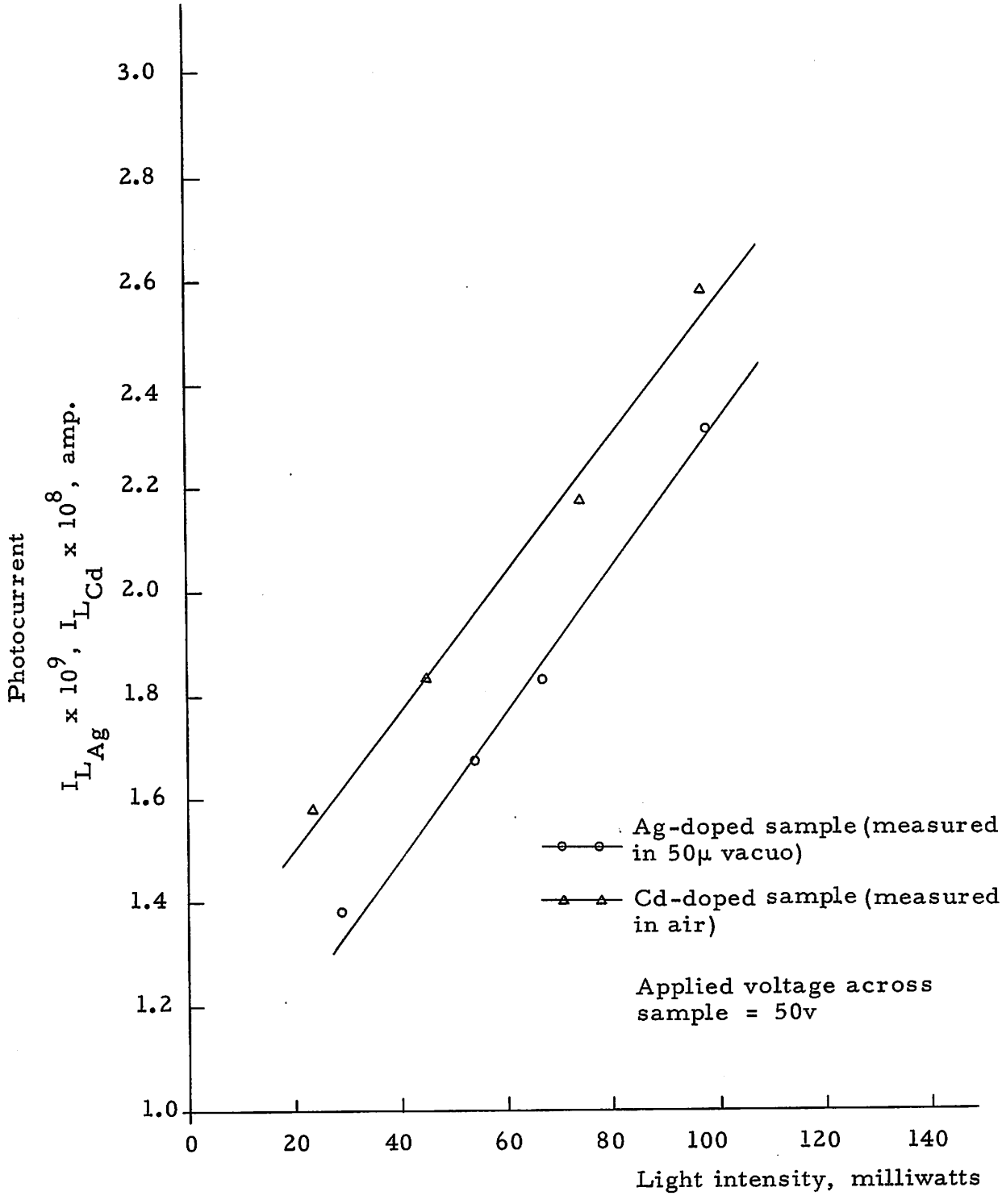

Fig. 18. Photocurrent vs light intensity

Table 3.

Photoconduction Characteristics of a Ag-doped Polymer Membrane

$I_D = 1.11 \times 10^{-9}$ amp, $\sigma_D = 2.56 \times 10^{-9} \Omega^{-1}\text{-cm}^{-1}$, $\tau = 29$ sec

$$i(t) = I_D + I_{ph}(1 - e^{-t/\tau})$$

$$\sigma(t) = \sigma_D + (\sigma_L - \sigma_D)(1 - e^{-t/\tau}) \qquad (10)$$

Light Intensity, mW	I_L, amp	Illuminated Conductivity, $\sigma_L \Omega^{-1}\text{-cm}^{-1}$	I_{ph}, amp
28	1.38×10^{-9}	3.18×10^{-9}	$.27 \times 10^{-9}$
54	1.68×10^{-9}	3.87×10^{-9}	$.57 \times 10^{-9}$
67	1.83×10^{-9}	4.21×10^{-9}	$.72 \times 10^{-9}$
99	2.31×10^{-9}	5.31×10^{-9}	1.20×10^{-9}

Both the dark and illuminated conduction current as a function of applied voltage were found to be ohmic up to 400 V; the results are plotted in Fig. 19.

Since a monochromatic light source was not available, the spectral response of the photocurrent was not investigated. However, it was demonstrated qualitatively that the photocurrent was a function of incident light frequency by observing the change in magnitude of photocurrent in different colors of light. A set of color filters* was used in the experiment. The results are tabulated in Table 4.

* Baird-Atomic, Inc.

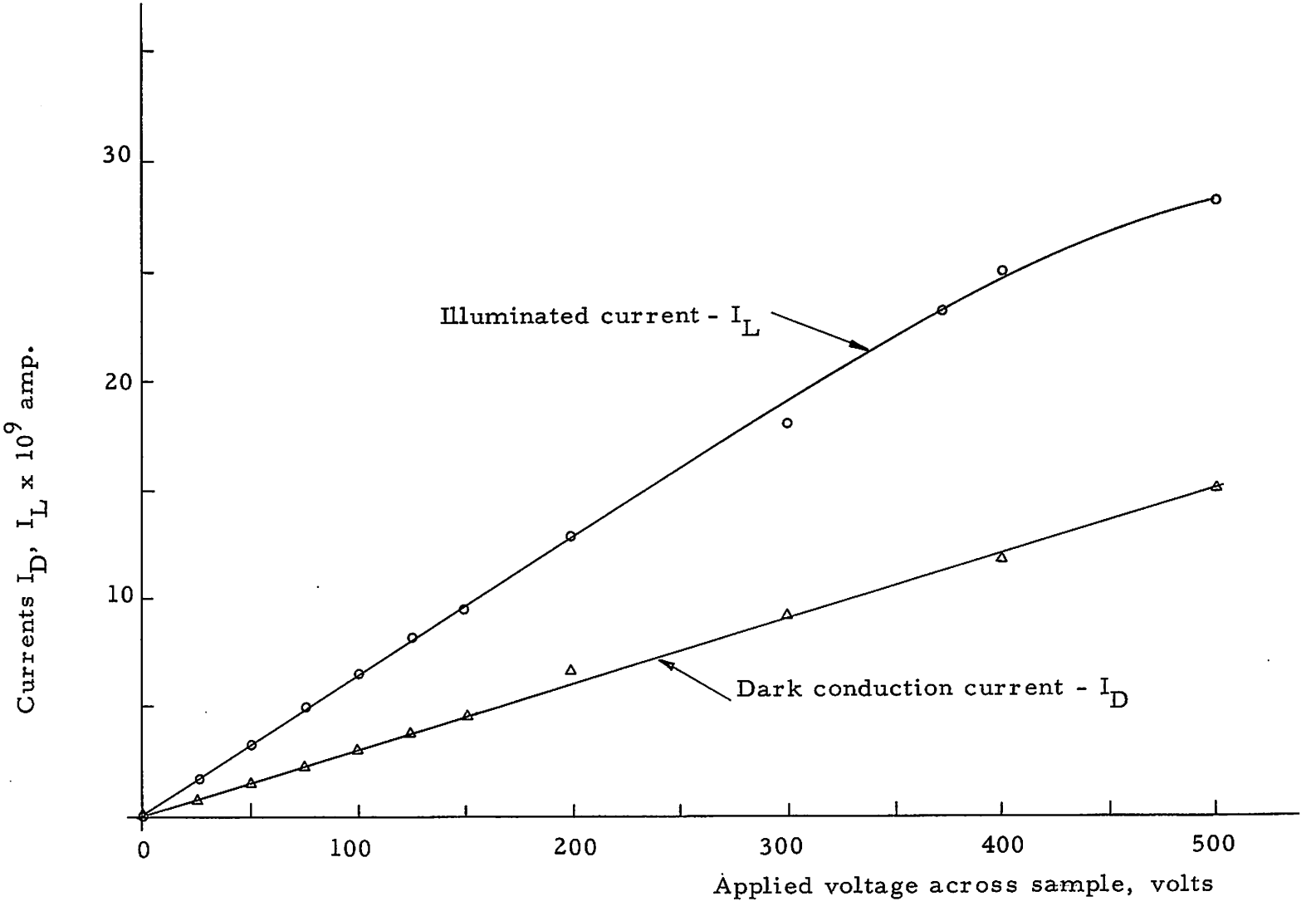

Fig. 19. Dark conduction current and photocurrent as a function of applied voltage (Ag-doped membrane)

Table 4.

Effect of Color Filters on Photocurrent in Ag-doped Polymer Membrane

Filter	Illuminated Current (I_L), amps
No Filter	2.67×10^{-9}
Dark Current	0.99
Red	1.98
Yellowish Green	2.16
Dark Green	1.29
Blue	1.35
Light Blue	1.50
Orange	2.22

The photoconduction characteristics of a Cd-doped membrane was first measured in air and then in vacuo. The response in air was similar to that in the Ag-doped form, except with a faster time constant of 6.7 sec. The results are plotted in Figs. 18 and 20.

The rise and decay of photocurrent in a Cd-doped membrane seemed to exhibit a different form in vacuo as shown in Figure 21. The response of a second order system to a step input was plotted on the same figure for comparison. Such a system is characterized by a differential equation of the form[19]:

$$\frac{1}{a^2}\frac{d^2i}{dt^2} + \frac{2b}{a}\frac{di}{dt} + i = r(t) \qquad (11)$$

where r(t) is the input function, and a and b are constants.

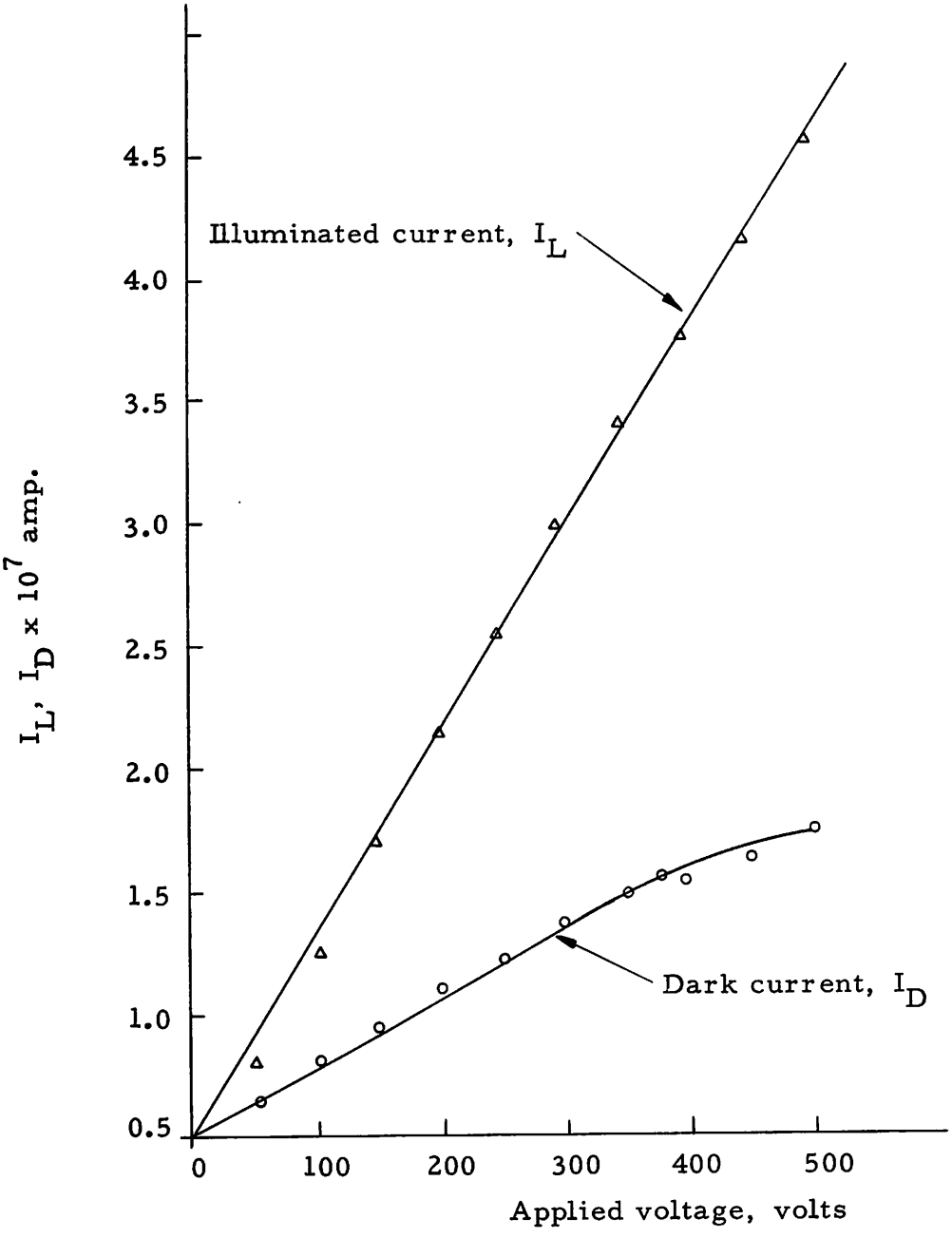

Fig. 20. Dark current and photocurrent vs applied voltage in Cd-doped membrane (measured in air)

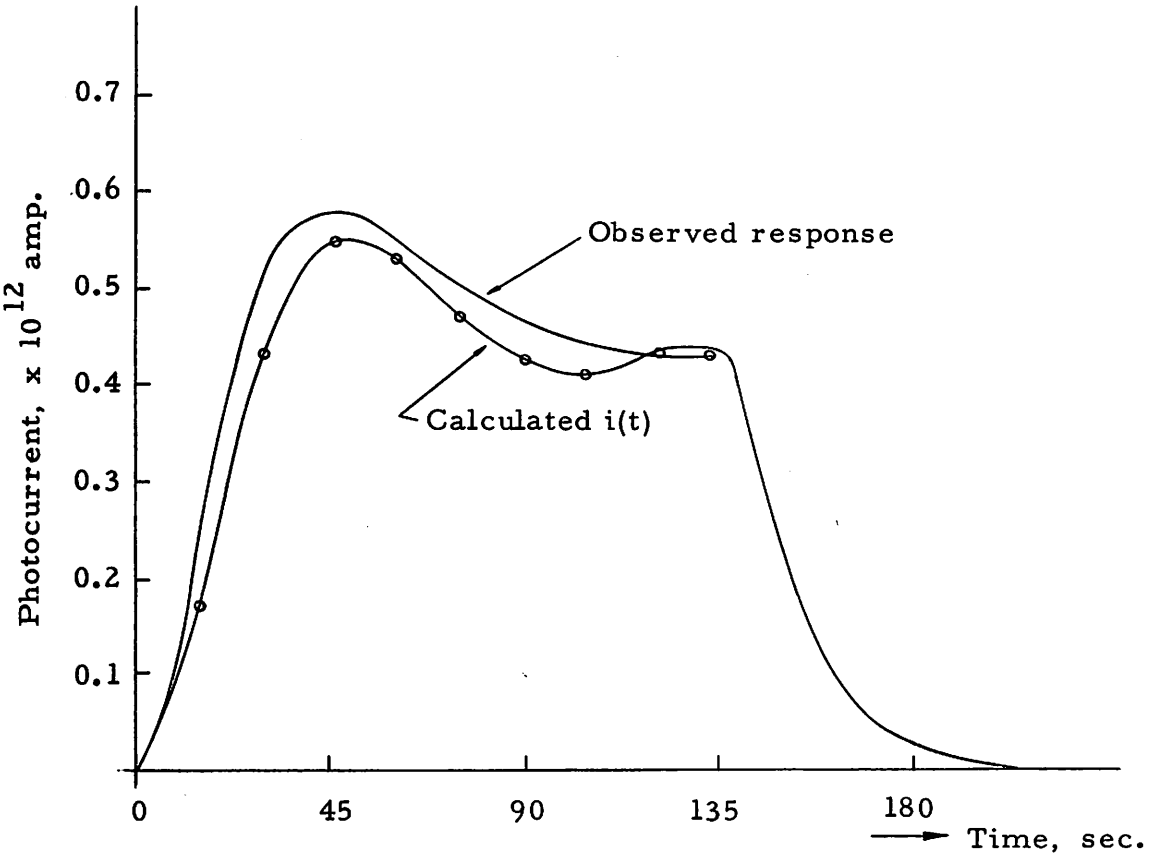

Fig. 21. Response of photocurrent in Cd-doped polymer membrane under dc illumination (in 50μ vacuo).

Considering r(t) as a step input of light, the solution to (11) is:

$$i(t) = I_{ph}\left(1 - \frac{e^{-abt}}{\sqrt{1 - b^2}} \sin\left(a\sqrt{1 - b^2}\, t + \cos^{-1} b\right)\right) \qquad (12)$$

The constants chosen to fit the curve were

$$a = 7.0 \times 10^{-2} \qquad b = 0.4$$

and we then have

$$i(t) = I_{ph}\left[1 - 1.1e^{-2.8\times10^{-2}t} \sin(3.7t + 66^{o})\right] \qquad (13)$$

IV. DISCUSSION OF RESULTS

A. CONDUCTION MODEL

The observed conductivities in the wet state for the different ionic forms are in the same order of magnitude and are several orders of magnitude higher than the corresponding conductivities in the dry state. It is believed that conduction in the wet state is ionic and the charge carriers are probably protons. A possible mechanism for protron transfer is:

$$2H_2O \rightleftharpoons H_3O^+ + OH^- . \qquad (14)$$

For membranes equilibrated in 50 micron vacuo, the samples can be considered as dry and the role of water in conduction mechanism can be neglected. It is also assumed that the polyethylene support matrix does not contribute to the conductivity since its specific conductivity is less than 10^{-15} ohm^{-1}-cm^{-1}.[20] Doping with different metallic ions has an insignificant effect on the values of σ except in the case of Cd, which is divalent while all others are monovalent. Each ionic form shows a characteristic activation energy.

In this discussion, it is assume that the conduction electrons are π electrons[21, 22] from the benzene ring structure in the PSA, and the metallic ions act as additional paths or bridges for intermolecular electron transfer. The charge transport then involves the transfer of electrons from one monomer to another or from the ring structure to the ionic sites and then onto the next monomer unit. Denoting each neutral monomer unit as X where

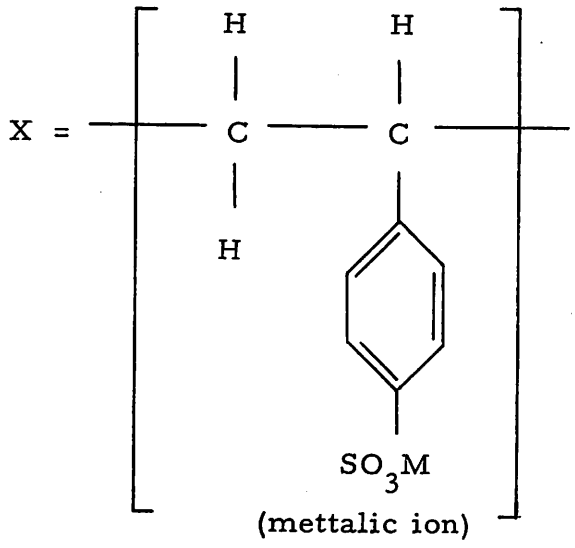

(15)

The electron transfer between monomer units can then be depicted as:

$$2X \rightleftharpoons X^+ + X^- , \tag{16}$$

which is analogous to the proton transfer in water as expressed in (14). Process (16) can occur by electrons hopping along the carbon chain or by the formation of intermediate charge transfer complexes involving the ionic sites. A conduction scheme by electron hopping process can be illustrated as follows:

$\mathcal{E}$ direction of applied field

$$\underset{1}{X}\ \underset{2}{X}\ \underset{3}{X}\ \underset{4}{X}\ \underset{5}{X}\ \underset{6}{X} \rightleftharpoons X^+\ X^-\ X\ X\ X\ X \rightarrow X\ X\ X^-\ X\ X\ X \tag{17}$$

Consider the ideal case that the chain ends are in contact with a pair of electrodes and the polarity of the applied potential as shown. Through thermal or optical excitation, an electron is transferred from monomer no. 1 to monomer no. 2. In the next step, the electron at no. 2 hops to no. 3 in the applied field, and an electron injected from the cathode recombines with the hole at no. 1. By repeating the process, a net

transfer of electrons down the chain is achieved. The polymer chain can be considered as an array of potential wells, each of which is associated with a monomer unit. Then for an electron to pass from one monomer unit to another, it must have enough energy to surmount the energy barrier; this energy can be acquired through thermal or optical excitation. Assuming that the PSA chains are in closed contact (in the order of atomic distances), at least at one point along their length with another, this array of potential well picture can be extended throughout the entire sample.

If the electron jumps occur via the ionic sites, the electron will spend some time at the positive ionic sites, and can be considered as trapping centers for the electrons. The motion of electrons in an applied field then consists of successive jumps between traps. The trapping effect will depend on the valence of the metallic ion that replaced the hydrogen. For example, the trapping effect will be much stronger for a divalent metal than for a monovalent one. For a divalent metal replacing the hydrogen, it will be necessary for the metallic ion to share between two sulfonic acid groups creating defects in the polymer chain, or if the divalent ion is bonded to only one sulfonic acid group (this can occur in the case of excess cation nonstoichiometry), a net positive charge remaining on the ion will become a strong electron trap. Defects created by a monovalent metallic ion in the polymer chain will be less significant. This valence dependent trapping is reflected in the higher activation energy, lower conductivity, and faster photocurrent time constant of the Cd-doped sample.

The mathematical treatment of the hopping process involves parameters unknown for the material under investigation. However, the mobility of charge carriers in an applied field as derived by Boltaks[22] will be given here indicating the factors involved.

$$\mu = \delta^2 \nu_0 \frac{q}{2kT} \exp(-E_\rho/kT) \qquad (18)$$

where

δ = periodic distance between potential wells, can be interpreted as center to center distance between monomer units,

ν_0 = frequency of approach of the electron to the potential barrier,

q = electronic charge,

k = Boltzmann's constant,

T = temperature in ^{o}K, and

E_ρ = height of potential barrier in eV, can be interpreted as the activation energy observed in the experiment.

Using the relationship

$$\sigma = n\mu q , \tag{19}$$

we have

$$\sigma = \frac{nq^2}{2kT} \delta^2 \nu_0 \exp(-E_\rho/kT) , \tag{20}$$

where

n = density of mobile conduction electrons.

The anisotropy of the conduction process can be treated by inserting a pre-exponential geometric factor,[9] A, which varies with the orientation of the PSA chains in the sample.

$$\sigma = A \cdot \frac{nq^2}{2kT} \delta^2 \nu_0 \exp(-E_\rho/kT) \tag{21}$$

The temperature dependence of $1/T$ over the temperature range of interest is insignificant comparing with that of $\exp(-E_\rho/kT)$, for E in the order of approx. 1 eV. Equation (21) can then be simplified to:

$$\sigma = A \cdot \sigma_0 \exp(-E_\rho/kT) . \qquad (22)$$

Therefore, a log σ vs 1/T plot will be a straight line. The observed experimental data agreed with this formulation.

In the measurement of conductivity anisotropy of Ag-doped membrane, E_ρ was found to be the same for all three directions; it shows that the anisotropic effect is related to the pre-exponential term as postulated. Anisotropy is probably caused by directional dependence of σ and ν_0, but the height of the potential barrier remains the same in all directions. In terms of measurable parameters, the mobility of the carriers is anisotropic.

B. HALL EFFECT

Failure to detect a Hall signal can be attributed to the low mobility of the carriers or to the hopping nature of the conduction process. In the Hall-effect phenomenon, a moving charge follows a curved path in a magnetic field. Carriers tend to accumulate on one side of the specimen which leads to buildup of the Hall voltage to counteract this transverse current flow. But if the charge carriers move by hopping, or traps are present, the distance and time they actually move are small and no significant deflection occurs in a magnetic field. Therefore, the Hall voltage is either too small to detect or does not exist. Techniques for measuring Hall signals in high resistivity materials have been devised by Fisher[24] and Heilmeier.[25]

C. PHOTOCONDUCTIVITY

Photoconduction is produced by the increase in charge carriers released in the material by photoexcitation. The vehavior of the material studied is very similar to a certain class of organic dyes observed by Vartanian,[26] and is characterized by an exponential rise and decay of photocurrent with a time constant of several seconds.

Consider a simple model in which the π electrons in the PSA chains are excited into their conduction state by irradiation with an external light source, creating electron-hole pairs. A fraction of the metal ionic sites are considered as trapping centers providing n_t electron trap levels per unit volume. We further assume that the holes

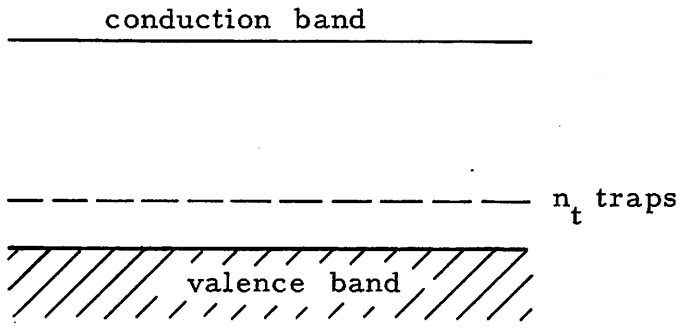

have very low mobility and the current carriers are predominantly electrons. Let Δn denote the excess electrons released by photoexcitation, then the rate of generation of carriers is given by[27]

$$\frac{d\Delta n}{dt} = L - R\,\Delta n(\Delta n + n_t) + Bn_t\,, \qquad (23)$$

where

L = number of photons absorbed per unit volume per unit time,

R = recombination coefficient, and

Bn_t = rate of thermal evaporation of trapped carriers back into the conduction band.

The term Bn_t can be neglected if the trap level is considered much closer to the valence band than to the conduction band, then (23) becomes

$$\frac{d\,\Delta n}{dt} = L - R\,\Delta n(\Delta n + n_t)\,. \tag{24}$$

In the steady state (24) is reduced to

$$\Delta n_s(\Delta n_s + n_t) = L/R\,, \tag{25}$$

where

Δn_s = photo-generated electrons in the steady state.

From Fadley's[11] calculation, the number of ionic sites is $\sim 10^{21}$/c.c. Assuming only a fraction of these sites act as trapping centers, this will still be much greater than Δn_s for the current level observed in this experiment. Therefore, in the limit $n_t >> \Delta n_s$,

$$\Delta n_s = L/Rn_t\,. \tag{26}$$

Since

$$I_{ph} = a\,q\,\mu\,\mathcal{E}\,\Delta n_s\,, \tag{27}$$

and L is proportional to light intensity, I_{ph} is also proportional to the intensity of illumination. The total illuminated current is the superposition of the dark current and the photocurrent

$$I_L = I_D + I_{ph} = a\,q\,\mu\,\mathcal{E}(n_0 + \Delta n_s)\,, \tag{28}$$

where

a = cross-sectional area of sample,

μ = mobility of carriers,

$\mathcal{E}$ = applied electric field,

n_0 = carrier concentration in the dark state,

I_D = dark conduction current,

I_L = steady state illuminated current, and

I_{ph} = steady state photocurrent.

Equation (28) checks with the empirical Eq. (8) reduced to the steady state. This model predicts that the photocurrent varies linearly with light intensity and is ohmic with the applied field; the agreement with experimental data is good, but ohmicity is observed only up to 400 V.

The response of the system on turning off the light is given by the transient solution of Eq. (24).

$$\log \frac{\Delta n + n_t}{\Delta n} - \log \frac{\Delta n + n_t}{\Delta n_s} = n_t R t \,. \tag{29}$$

For the case of $n_t >> \Delta n$, the solution reduces to

$$\Delta n = \Delta n_s \, e^{-n_t R t} \,. \tag{30}$$

Multiplying Eq. (3) by $a q \mu \mathcal{E}$

$$i_{ph}(t) = I_{ph} \, e^{-n_t R t} \,. \tag{31}$$

Adding the dark current we have,

$$i(t) = I_D + I_{ph} \, e^{-n_t R t} \,. \tag{32}$$

Let

$$\tau = \frac{1}{n_t R} \cdot \tag{33}$$

It can be seen that i(t) has the same form as the empirical Eq. (9). The rise of illuminated current is given by:

$$i(t) = I_D + I_{ph}\left(1 - e^{-n_t R t}\right) \tag{34}$$

From Eq. (33) it can be deduced that the rate constant is inversely proportional to the trapping effect, this is verified by the shorter time constant observed with the Cd-doped membrane. The stronger trapping effect caused by Cd ions than by Ag ions is discussed in Sec. IV part (A).

The nature of response in the Cd-doped membrane upon prolonged outgassing indicated a second order kinetics system. This can be postulated as follows. If an electron freed from a trap has a higher probability to recombine than to be retrapped, the initial response will be of first order. If the probability of retrapping is higher than to recombine, the process will be of second order.[28] This is plausible due to the strong trapping action at the Cd ion sites.

V. CONCLUSION

A well-defined theory concerning the charge-transport mechanism in organic semiconductors remains elusive. One of the two main approaches for interpreting the experimental data is to apply the band theory assuming the carriers travel in a wave-like fashion through the lattice. An alternative approach is to visualize the charge transport mechanism as thermally activated, random hopping motion of the charge carriers between neighboring lattice sites. The hopping model seems to work well in interpreting the data of this experiment. For better understanding of the conduction process, it would be desirable to try to determine the sign of charge carriers by thermoelectric effect or gas ambients.

The application or organic semiconductors in actual devices is still in its infancy. Rectifying effects in polymers has been reported by Vannikov.[29] Attempts to make the photosensitivity of polymers to approach that of inorganic photoconductors like zinc oxide and selenium by using different dopants have been tried by Hoegl.[30] Semiconductive films and coatings are valuable in corrosion control and in electrostatically sensitized photography. Polymers with their light weight, mechanical flexibility, and wide range of electrical characteristics can be promising in future applications.

REFERENCES

1. D. D. Eley, Nature, 162, 819 (1948).
2. D. D. Eley, and G. D. Parfitt, Trans. Faraday Soc., 51, 1529 (1955).
3. H. Inokuchi, and H. Akamatu, "Electrical conductivity of organic semiconductors," Solid State Physics - Advances in Research and Applications, vol. 12, Academic Press 1961.
4. A. Szent-Gyorgyi, Nature, 157, 875 (1946).
5. B. Rosenberg, J. Chem. Phys., 36, No. 3, p. 816, (1962).
6. W. Arnold, "An electron-hole picture of photosynthesis," J. Phys. Chem., 69, No. 3, (1965).
7. "Organic semiconductors," Chem. Eng. News, 40, No. 9, (1962).
8. J. H. Lupinski, and K. D. Kopple, "Electroconductive polymers," Science, vol. 146, p. 1038, No.v, 1964.
9. H. A. Pohl, "Semiconduction in polymers (A Review), " Tech. Rept. 61D, (1961), Plastics Lab., Princeton University.
10. J. F. A Hazenberg, and B. P. Knol, U. S. Patent No. 3,133,889, May 19, 1964.
11. C. S. Fadley, "Electrical conductivity and ionic transport phenomena in a polycationic membrane," M.S. Thesis, Univ. of Calif., Berkeley, Jan. 1965.
12. V. P. Dobrego, and S. M. Ryvki, "Photoconductivity by a hopping process," Soviet Phys. - Solid State, 6, No. 4, Oct. 1964.
13. E. H. Putley, "The Hall effect and related phenomena," Butterworth, 1960.
14. A. Bree, and P. J. Reucroft, "Trapping centers and electronics conduction processes in anthracene," Symposium on Electrical Conductivity in Organic Solids, Interscience Publishers, 1961.
15. R. Sehr et al., "Semiconductive properties of molecular complexes," Symposium on Electrical Conductivity in Organic Solids, Interscience Publishers, 1961.
16. R. W. Smith, and A. Rose, Phys. Rev., 97, 1531, (1955).

17. N. Riehl, Symposium on Electrical Conductivity in Organic Solids, Interscience Publishes, p. 61, 1961.

18. N. E. Mott, and R. W. Gurney, Electronic Processes in Ionic Crystals, p. 172, Oxford Univ. Press, (1940).

19. D'azzo and Houpis, Feedback Control System Analysis and Synthesis, McGraw Hill Book Co., Inc., New York, p. 58, (1960).

20. Handbook of Chemistry and Physics, p. 1554, 43rd Edition, Chemical Rubber Publishing Co., 1961.

21. C. B. Garrett, chap. 15, Semiconductors, edited by N. B. Hannay, Rheinhold Publishing Corp., N. Y. (1959).

22. L. V. Azariff, and J. J. Brophy, Electronic Processes in Materials, p. 262, McGraw Hill Book Co., Inc., New York, 1963.

23. B. I. Boltaks, Diffusion in Semiconductors, chap. 3, Academic Press, 1963.

24. Fisher et al, "Apparatus for the measurement of galvanomagnetic effects in high resistivity semiconductors," Rev. Sci. Instr., 32, no. 7, 1961.

25. G. H. Heilmeier et al., "Integrating the Hall signal out of noise," Phys. Rev. Letters, 8, 309 (1962).

26. A Terenin, "Photoelectric properties of semiconducing organic dyes," Symposium on Electrical Conductivity in Solids, p. 39, Inserscience, (1961).,

27. C. Kittel, chap. 18, Introduction to Solid State Physics, John Wiley & Sons, 1962.

28. R. C. Nelson, J. Chem. Phys., 22, No. 5, 1954.

29. A. V. Vannikov, Doklady Akad. Nauk S.S.S.R., 152(4), 905-7, (1963).

30. H. Hoegl, J. Phys. Chem., 69, no. 3, 1965.